Composite short-side-chain PFSA electrolyte membranes containing selectively modified halloysite nanotubes (HNTs)

Sahng Hyuck Woo, Aurélie Taguet, Belkacem Otazaghine, Alia Akrout, Sara Cavaliere, Arnaud Rigacci, Christian Beauger

Composite short-side-chain PFSA electrolyte membranes containing selectively modified halloysite nanotubes (HNTs)

Sahng Hyuck Woo[1,2], Aurélie Taguet[3], Belkacem Otazaghine[3], Alia Akrout[4], Sara Cavaliere[4,5], Arnaud Rigacci[1], and Christian Beauger[1,*]

[1] *MINES ParisTech, Center for Processes, Renewable Energy and Energy Systems (PERSEE), PSL University, CS10207 rue Claude Daunesse, 06904 Sophia Antipolis Cedex, France*

[2] *Laboratory for Marine Energy Convergence and Integration, Korea Institute of Energy Research (KIER), 200 Haemajihaean-ro, Gujwa-eup, Jeju-si, Jeju-do 63359, Republic of Korea*

[3] *Centre des Matériaux des Mines d'ales (C2MA), IMT – Mines Alès, 6 Avenue de Clavières, 30319 Ales Cedex, France*

[4] *Agrégats Interfaces et Matériaux pour l'Energie, ICGM, CNRS, ENSCM, Université de Montpellier, 34095 Montpellier Cedex 5, France*

[5] *Institut Universitaire de France (IUF), Paris, France*

ABSTRACT

Aquivion membrane displays improved properties as compared to Nafion membrane, partly due to shorter side chains. However, some improvements are still necessary for proton exchange membrane fuel cell to operate at low relative humidity. To overcome this drawback, the addition of clay nanoparticle into the Aquivion matrix can be considered. In this study, different composite mem-branes have been prepared mixing short-side-chain PFSA (perfluorosulfonic acid) Aquivion and selectively modified halloysite nanotubes for PEMFC low relative humidity operation. Halloysites were grafted with fluorinated groups, sulfonated groups, or perfluoro-sulfonated groups on inner or outer surface of the tubes. The obtained composite membranes showed improved properties, especially higher water uptake associated with reduced swelling and better mechanical strength compared to pristine Aquivion membrane and commer-cially available Nafion HP used as reference. The best performance in this study was obtained with Aquivion loaded with 5 wt% of pretreated perfluoro-sul-fonated halloysite. The composite membrane, referred to as Aq/pHNT-SF5, displayed the largest water uptake and proton conductivity among the panel of membranes tested. The chemical stability was not affected by the presence of halloysite in the Aquivion matrix.

Address correspondence to E-mail: christian.beauger@mines-paristech.fr

GRAPHICAL ABSTRACT

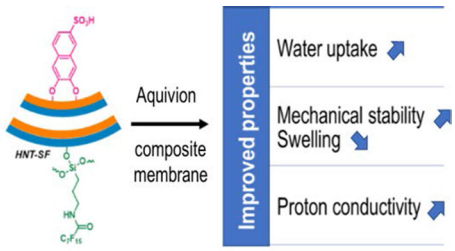

Introduction

Proton exchange membrane fuel cells (PEMFC) are efficient energy conversion devices potentially environmentally friendly. Among the wide range of ionomers used to prepare proton exchange membranes (PEMs), Nafion has been widely selected due to its excellent proton conductivity and rather good thermal and mechanical stability at low temperature [1]. The limited operating conditions of Nafion membranes urge the community to search for alternatives performing at higher temperature and lower relative humidity. Aquivion is a short side chain PFSA ionomer, adopted for its enhanced thermal stability and proton conductivity compared to those of Nafion, resulting from higher glass transition temperature, generally lower equivalent weight, and larger crystallinity [2, 3]. Aquivion membranes show also improved chemical stability and can operate at higher temperatures than Nafion membranes, due to better thermo-mechanical characteristics [4]. It was demonstrated, through endurance tests conducted for 500 h, that Aquivion membranes can be operated up to 110 °C, which is 15 °C higher than Nafion membrane [5]. Increasing the operating temperature of PEMFCs results in better carbon monoxide (CO) tolerance, easier heat management, on top of better reaction kinetics during operation. That is, fuel cell operation at high temperature reduces CO adsorption on Pt, makes the generated heat more valuable and releases constraints on cooling the stack [6, 7].

PFSA alone is not suitable to operate at low relative humidity. Hence, various inorganic fillers have been used as additives to enhance the physicochemical properties of membrane electrolytes for use in PEMFC. Adding inorganic fillers into the polymer matrix can improve the hygroscopicity and mechanical strength of the membrane, the hydrogen crossover and even the proton conductivity. For instance, zeolites such as NaA zeolite, ETS-10, umbite, mordenite, analcime, faujasite, b-zeolite, ZrP-modified zeolite, and H-type of b-zeolite [8–13]; inorganic oxides such as TiO_2, SiO_2, ZrO_2, and ZrO_2/SO_4^{2-} [8, 14–24]; and montmorillonite, laponite, sepiolite, and halloysite [8, 9, 25–33] have been studied for long time.

The addition of nanoclay into the polymer matrix can overcome the limitations associated with thermomechanical resistance and sensitivity to relative humidity, even when operating at high temperatures. Preparing composite membranes embedding nanoclays prevents dehydration, especially by improving water retention allowing operation at low relative humidity [34, 35]. Mechanical properties can be also improved by a homogenous dispersion of the fillers, a better affinity with the polymer used in the composite membrane, or exfoliation in the case of some lamellar nanoclays [33, 36]. Moreover, the addition of fillers can reduce the occurrence of hydrogen crossover during operation [35].

Halloysite is a natural nanoclay, composed of nanotubes formed by tetrahedral silica and octahedral alumina units in external and internal layers, respectively. Resulting from their 1D morphology, the tensile strength of the composite membrane can

be enhanced through reinforcement [37, 38]. In some cases, however, aggregated nanoclays can decline the performance of the composites. Hence, research groups have developed various methods to improve the dispersion state, interface, and proton conductivity of ionomer/halloysite nanotube composite, for example by surface modification such as sulfonation [37, 39–41], amination [37, 41–43], or impregnation with phosphotungstic acid (PWA) [44]. Optimizing the blending time of the casting dispersion is also of major importance [45].

To date, the influence of halloysite nanotubes inside Aquivion electrolyte membranes has not been fully investigated for PEMFC applications. Moreover, it has not been fully evidenced that selective chemical modification of the halloysite surface can improve some physicochemical properties regarding Aquivion composite membranes. In particular, the sulfonic acid on the inner surface made protons easier to move inside the composite membrane. If so, this approach will be of significant benefit for the PEMFC to operate over a wide range of conditions.

The present study focuses on novel halloysite nanotube-based Aquivion composite membranes to be operated at low relative humidity. To achieve this approach, sulfonation and fluorination were selected on the inner and outer surface of halloysite fillers, respectively. We demonstrated that the addition of functionalized and pretreated halloysites into Aquivion dispersion enhanced the physicochemical properties of the resulting composite membranes compared to those of non-modified membranes and commercially available Nafion HP (Nafion, 23 μm thick). The comparison was based on several properties (composite homogeneity, water uptake, dimensional stability, ion exchange capacity and proton conductivity but also mechanical strength as well as chemical stability) characterized in a range of conditions of temperature and relative humidity.

Experimental

Materials

Halloysite nanotubes were obtained from Sigma Aldrich. Sodium 2,3-dihydroxynaphthalene-6-sulfonate and *N*-(3-triethoxysilylpropyl)perfluorooctanoamide were purchased from ABCR. Ethanol, acetone and tetrahydrofuran (THF) were purchased from Fisher Chemical. All these products were used for functionalization without further purification.

Aquivion (24%, D83-24B) was purchased from Solvay. Hydrogen peroxide (H_2O_2, 30%) and oxalic acid (0.45 M) were purchased from Fisher Scientific, UK. Sulfuric acid (H_2SO_4, 5 N), sodium hydroxide (NaOH, 98%) and hydrogen chloride (HCl, 0.1 N) were purchased from Alfa Aesar, Germany. Total ionic strength adjustment buffer solution (TISAB IV) and sodium fluoride (NaF) were purchased from Sigma Aldrich. Sodium chloride (NaCl, 99.5%) and isopropanol (99.5%) were purchased from Acros Organics. Deionized (DI) water (18.2 MΩ cm) was supplied from ultrapure water plants (Smart2Pure, Thermo Scientific).

Experimental methods

Halloysite fluorination (HNT-F)—Scheme 1

Into a 250 mL flask fitted with a condenser, the following materials were introduced to obtain HNT-F clay nanoparticles: 10 g of halloysite, 1 g (1.6×10^{-3} mol) of *N*-(3-triethoxysilylpropyl)perfluorooctanoamide and 100 mL of an ethanol/water (90/10 wt%) solution. The mixture was then stirred and heated at solvent reflux for 15 h. The mixture was next centrifuged (5000 rpm) to eliminate the liquid phase and washed twice with acetone and THF. Finally, the modified filler was dried under vacuum and ground before characterization.

Halloysite sulfonation (HNT-S)—Scheme 1

Into a 250 mL flask fitted with a condenser, the following materials were introduced to obtain HNT-S clay nanoparticles: 10 g of halloysite, 1 g (3.8×10^{-3} mol) of sodium 2,3-dihydroxynaphthalene-6-sulfonate and 100 mL of deionized water. The mixture was then stirred and heated at solvent reflux for 15 h. The mixture was next centrifuged (5000 rpm) to eliminate the liquid phase and washed twice with water and acetone. Finally, the modified filler was dried under vacuum and ground before characterization.

Halloysite perfluoro-sulfonation (HNT-SF)—Scheme 1

Into a 250 mL flask fitted with a condenser, the following materials were introduced to obtain HNT-SF clay nanoparticles: 10 g of sulfonated halloysite previously obtained, 1 g (1.6×10^{-3} mol) of *N*-(3-

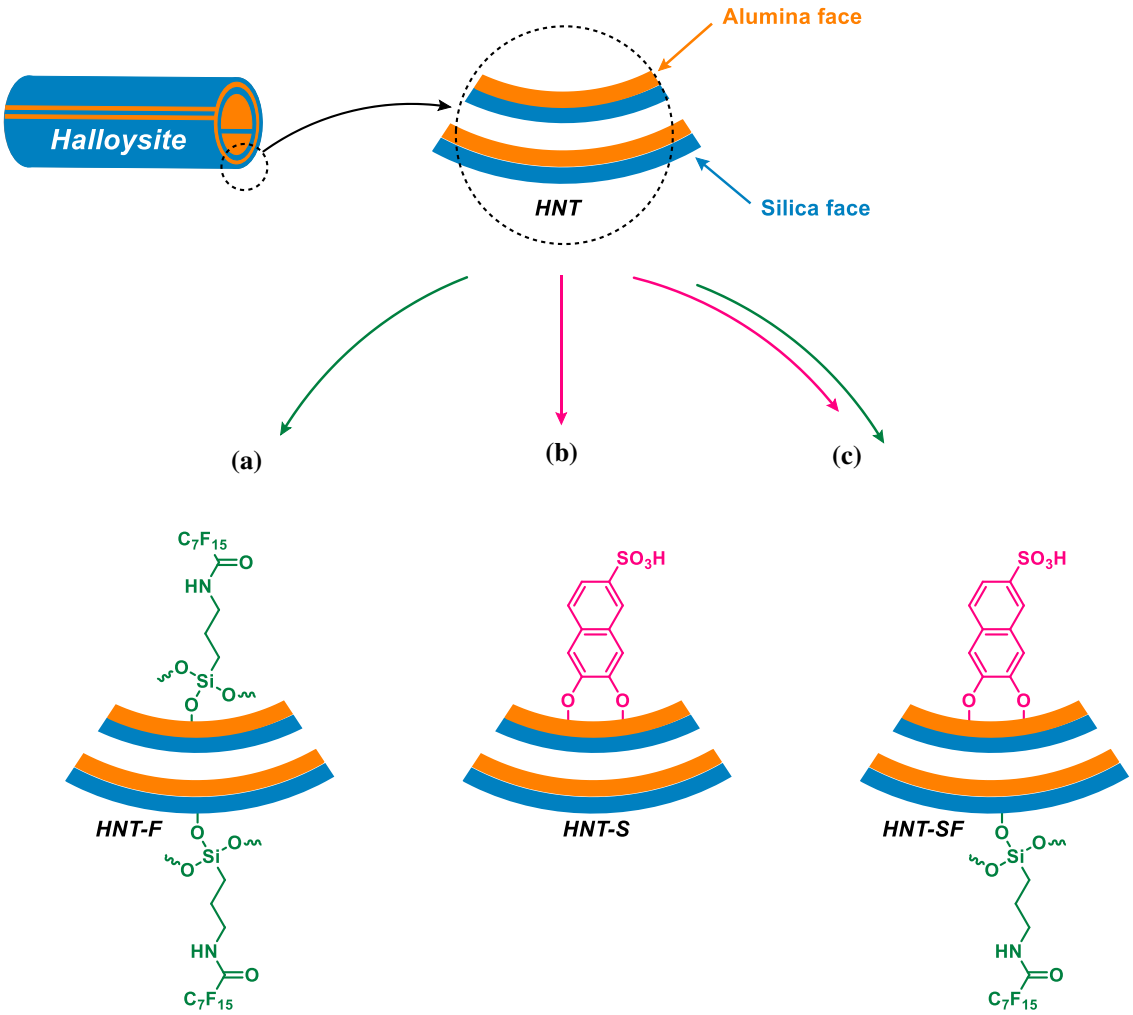

Scheme 1 Schematic representation of halloysite nanotube functionalization. The silanol (Si–OH) and aluminol (Al–OH) groups of halloysite nanotube were combined with a fluorinated, b sulfonated and c perfluoro-sulfonated monomers via a condensation reaction. As for perfluoro-sulfonated halloysites, the sulfonated halloysite previously obtained (i.e., HNT-S), followed by functionalizing *N*-(3-triethoxysilylpropyl)perfluorooctanoamide.

triethoxysilylpropyl)perfluorooctanoamide and 100 mL of an ethanol/water (90/10 wt%) solution. The mixture was then stirred and heated at solvent reflux for 15 h. The mixture was next centrifuged (5000 rpm) to eliminate the liquid phase and washed twice with acetone and THF. Finally, the modified filler was dried under vacuum and ground before characterization.

Pretreatment of halloysite nanotubes

A specific pretreatment was applied to halloysite nanotubes in order to eliminate most of the iron it may contain, which may affect the chemical stability of the PFSA membrane [46]. Each 1 g of pure halloysite and functionalized halloysite (i.e., HNT-F, HNT-S, or HNT-SF) were pretreated by stirring in 100 cm^3 of 0.5 M oxalic acid solution at 80 °C for 2.5 h. It was then filtrated using membrane filter (0.4 µm of pore size, Merck Millipore) and washed using DI-water. The halloysite was dispersed in DI-water using ultrasound (HD 2070, Bandelin, Germany) for 2 min at 60 W power and 20% pulsation lev. Finally, halloysite was treated with 0.001 M HCl solution under stirring at 80 °C for 2.5 h. Filtration and ultrasound were repeated under identical conditions. After that, pretreated HNT was precipitated in water and supernatant was removed. Finally, the pretreated halloysite was filtered and dehydrated overnight at

60 °C. Prefix *p* was added before HNT in the sample label.

Membrane preparation

For each kind, one or two 20 μm thick electrolyte membranes, 13 × 13 cm^2 in size, were prepared through casting—evaporation. Each of them was then cut into nine pieces of membrane. To begin with, 3.2 g of Aquivion dispersion (24%, D83-24B) was blended with 0.016 g (respectively, 0.039 g or 0.078 g) of pristine or modified halloysites and isopropanol (12.27 g) to prepare 2 wt% (respectively, 5 or 10 wt%) nanoclay loaded composite membranes. Casting dispersions used for membrane preparation were stirred for 15 min at 80 rpm and dispersed using an ultrasound micro-tip (HD 2200, Bandelin, Germany) for 2 min at 60 W power and 20% pulsation level. The resultant dispersions were poured in a mold and heated in an oven in two steps, 80 °C for 18 h and 170 °C for 2 h. Prepared membranes were finally treated in 0.5 M boiling H_2SO_4 for 1 h and then rinsed with DI-water for 1 h at 100 °C.

Table 1 summarizes the list of the prepared membranes. For nomenclature, Aq/HNT, Aq/HNT-F, Aq/HNT-S and Aq/HNT-SF represent composite membranes containing pristine, fluorinated, sulfonated and perfluoro-sulfonated halloysites, respectively. Prefix p means pretreated. More specifically, Aq/pHNT, Aq/pHNT-F, Aq/pHNT-S and Aq/pHNT-SF represent composite membranes incorporated with pretreated halloysite, pretreated—Fluorinated halloysite, pretreated—Sulfonated halloysite and pretreated—Perfluorosulfonated halloysite, respectively.

Analytical methods

ATR-FTIR

The surface modification of halloysite was investigated by Fourier transform infrared (FTIR) spectroscopy. FTIR was performed on a spectrometer IFS 66 (Bruker) and spectra were obtained by collecting 32 scans between 400 and 4000 cm^{-1} with a resolution of 4 cm^{-1}.

Py–GC/MS

Pyroprobe 5000 pyrolyzer (CDS analytical) was used to flash pyrolyze the samples in a helium environment. This pyrolyzer is equipped with an electrically heated platinum filament. One coil probe enables the pyrolysis of samples (< 1 mg) placed in a quartz tube between two pieces of rock wool. The sample was heated at 900 °C. The temperature was held for 15 s, and then the gases were drawn to the gas chromatograph for 5 min. The pyroprobe 5000 is interfaced to a 450-GC chromatograph (Varian) by means of a chamber heated at 270 °C. In the oven, the initial temperature of 70 °C was raised to 310 °C at 10 °C/min. The column is a Varian Vf-5 ms capillary column (30 m × 0.25 mm; thickness = 0.25 μm) and helium (1 *L*/min) was used as the carrier gas, a split ratio was set to 1:50. The gases were introduced from the GC transfer line to the ion trap analyzer of the 240-MS mass spectrometer (Varian) through the direct-coupled capillary column.

Table 1 List of the seventeen different kinds of membranes prepared (HNT, HNT-F, HNT-S, HNT-SF = pristine, fluorinated, sulfonated, perfluoro-sulfonated halloysite, 2/5/10 = nanoclay loading in wt%, *p* = pretreated halloysite (see "Halloysite perfluoro-sulfonation (HNT-SF)—Scheme 1" section))

Membrane label	Ionomer	Nanoclay reference/loading (wt%)	Modification of nanoclay	Acidic pretreatment of nanoclay
Aquivion	Aquivion	–	–	–
Aq/HNT	Aquivion	HNT10	Pristine	–
Aq/HNT-F		HNT-F10	Fluorination	–
Aq/HNT-S		HNT-S10	Sulfonation	–
Aq/HNT-SF		HNT-SF10	Sulfo + fluo	–
Aq/pHNT	Aquivion	pHNT2/5/10	Pristine	○
Aq/pHNT-F		pHNT-F2/5/10	Fluorination	○
Aq/pHNT-S		pHNT-S2/5/10	Sulfonation	○
Aq/pHNT-SF		pHNT-SF2/5/10	Sulfo + fluo	○

TGA

The thermal stability of the halloysite nanotubes was studied by thermogravimetric analysis (TGA). The analyses were performed by a thermogravimetric analyzer (Perkin Elmer Pyris-1 instrument). In order to remove all the physisorbed water, an isothermal step (10 min, 110 °C) was performed before the analysis and then the samples were heated to 900 °C at a heating rate of 10 °C/min. Measurements were carried out under nitrogen atmosphere with a flow rate of 20 mL/min on samples of approximately 10 mg.

FE-SEM and EDS

Cross section of prepared membranes was observed via FE-SEM (FEI XL30, Philips) at 2000 × magnification. Si/F atomic ratio (%) was calculated across the membrane section through EDS measurements, in order to follow the clay dispersion state within the polymer phase. In addition, Fe/Si atomic ratio (%) of halloysites was analyzed using EDS to confirm the removal of iron inside halloysite nanotubes pretreated by acidic solutions.

Membrane thickness

The wet membrane thickness was determined on seven different pieces using a micrometer (Mitutoyo 293–344, Japan) averaging measurements obtained at three different points of samples (center and two edges). A total of nine points were averaged per membrane type. The dry membrane thickness was assessed after FE-SEM cross section observation (average of three measurements).

Water uptake

The room temperature water uptake was measured by weight difference between wet and dried membranes. The membranes were first soaked in DI water to get their weight under wet conditions. The membranes were then dried in an oven at 80 °C for 18 h to obtain their weight under dry conditions. The water uptake of prepared membranes was calculated using the following equation:

$$W_{ut}(\%) = \frac{W_w - W_d}{W_d} \times 100 \quad (1)$$

where W_w and W_d are the weight of the wet and dried membranes, respectively.

Swelling ratio

Two kinds of membrane swelling were measured as the evolution of the membrane thickness between (1) dry and wet states at room temperature and (2) wet states after immersion 2 h in water at room temperature and 100 °C. The thickness of all membranes was averaged at three points, and the membrane swelling was calculated according to the following equations:

$$S_{th\_1}(\%) = \frac{th_{wet\_rt} - th_{dry\_rt}}{th_{dry\_rt}} \times 100 \quad (2)$$

$$S_{th\_2}(\%) = \frac{th_{wet\_bt} - th_{wet\_rt}}{th_{wet\_rt}} \times 100 \quad (3)$$

where th_{wet_rt} and th_{wet_bt} are the thickness of the wet membranes after immersion 2 h in water at room temperature and 100 °C, respectively. th_{dry_rt} represents the thickness of dried membranes.

Ion exchange capacity (IEC)

IEC was obtained through titration. The membrane's samples were fully immersed for 1 day in 2 M NaCl solution for Na^+ to replace H^+. Afterward, H^+ ions expulsed in the solution were titrated using a 0.005 M NaOH solution. IEC was calculated based on the following equation:

$$\text{IEC}\ (\text{meq/g}) = \frac{V_{NaOH} \times C_{NaOH}}{W_d} \quad (4)$$

where V_{NaOH} and C_{NaOH} are volume and concentration of NaOH, respectively. W_d is the weight of dried membranes.

Chemical stability

The presence of iron may be responsible for chemical degradation of the membranes during fuel cell operation through C–F bonds attacks [47]. Such a degradation will result in fluorine elution which can be followed through water chemical analysis. Hence, the chemical stability of membranes can be assessed via the analysis of the fluoride (F^-) concentration in the water produced during operation.

Pieces of wet membrane were immersed at 80 °C under stirring (100 rpm) in 4.4 M H_2O_2/1.25 mM H_2SO_4 solutions (using brown bottles) in order to

reach 0.16 wt%. Pieces were removed after 48 h, 72 h and 96 h of immersion, and the fluoride concentration of the solution was analyzed using an Ion meter (781 pH/Ion meter, Metrohm AG, Switzerland). TISAB IV was mixed with the aforementioned solution, and aliquots of 0.001 M NaF solution were used as a standard during analysis.

DMA (Dynamic mechanical analysis)

Dynamic mechanical analysis (DMA50 from Metravib, Acoem) was performed on pieces of membranes (30 mm × 10 mm × 40 µm thick) in order to evaluate their viscoelastic behavior, especially storage modulus and glass transition temperature. The measurements were performed under shear jaws for film test configuration. The results were analyzed with DYNATEST software.

Two different tests were performed. In the first test, after an isotherm of 10 min at 50 °C, a temperature scanning was performed on membranes from 50 to 180 °C at a heating rate of 1 °C/min, at a frequency of 1 Hz and at a deformation of 3 µm. Membranes were conditioned in a chamber at 50 °C and 50% RH prior to testing. In a second test, membranes were sheared at 50 °C and various relative humidity (around 15, 45 and 60% RH). The relative humidity was varied with a HG-10 humidity generator commercialized by Michell Instruments.

EIS (Electrochemical impedance spectroscopy)

The through-plane resistance of membranes was measured between two electrodes in a homemade cell, using electrochemical impedance spectroscopy (EIS, equipment Bio-Logic Scientific Instruments, France). The measurement temperature was set at 50 °C, 70 °C, or 90 °C, and the relative humidity was set at 25%, 50%, 75%, or 90%. The frequency was varied from 1 MHz to 1 kHz with an amplitude of ± 20 mV. All resistance values (Ohm) were calculated from 50 scans, by averaging high-frequency intercept of the impedance curve with the x axis (imaginary part equals zero). The through-plane proton conductivity (mS cm^{-1}) of membranes is then calculated based on the following equation:

$$\sigma = \left(\frac{1}{R}\right)\left(\frac{l}{S}\right) \quad (5)$$

where σ represents the proton conductivity (S cm^{-1}). R and l are the resistance (Ohm) and the thickness (cm) of the membrane, respectively. S represents the contact surface with electrodes (cm^2).

Results and discussion

Characterization of the fillers

Functionalization of halloysite nanotube (ATR-FTIR, TGA, Py–GC/MS)

FTIR was used to investigate the pristine and modified HNTs. As shown in Fig. 1, the different HNT samples show almost similar spectra. Characteristic peaks are observed at 3693 and 3628 cm^{-1}, assigned to the O–H stretching vibrations of inner-surface Si–OH and inner Al–OH, respectively [48]. The band for O–H deformation of inner Al–OH can also be

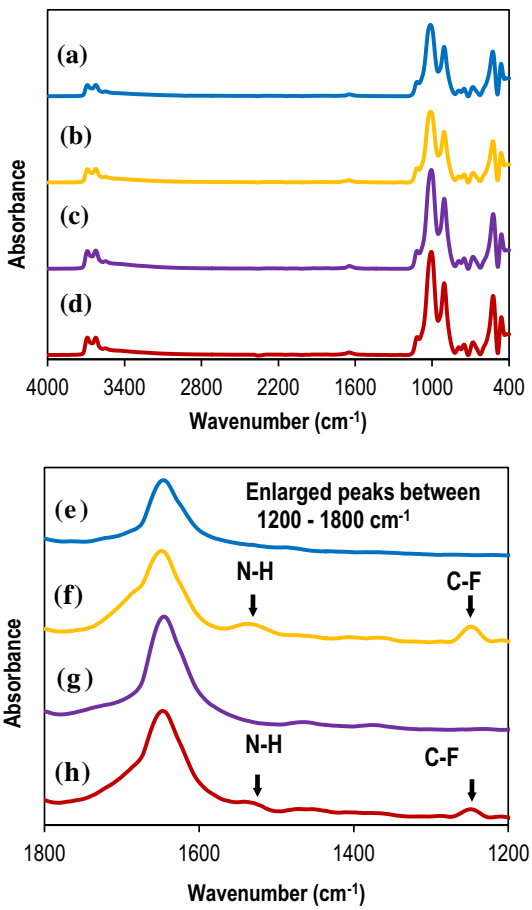

Figure 1 ATR-FTIR spectra of **a**, **e** pristine halloysite, **b**, **f** HNT-F, **c**, **g** HNT-S and **d**, **h** HNT-SF.

observed at 908 cm^{-1}. The band at 1647 cm^{-1} corresponds to strongly bending vibrations of the adsorbed water. The band at 1124 cm^{-1} is ascribed to the perpendicular Si–O stretching vibration, and the band at 1020 cm^{-1} can be assigned to in-plane Si–O stretching vibrations. The bands for deformations of Al–O–Si and Si–O–Si can also be observed at 530 and 465 cm^{-1}, respectively. Compared to the unmodified halloysite, the introduction of the fluorinated grafting agent onto halloysite surface results in the presence of some new peaks between 1200 and 1800 cm^{-1}. Indeed HNT-F and HNT-SF spectra show the presence of two peaks at 1535 and 1250 cm^{-1} attributed, respectively, to the N–H (bending) of the amide function and C–F bonds of the perfluorinated fragment. Moreover, the modification of the shape of the band centered at 1647 cm^{-1} (with an enlargement of the peak for the highest wave numbers) was attributed to the C=O stretching vibration of the amide function. Finally, the HNT-S spectrum does not show significant differences with that of HNT.

Thermogravimetric analyses were also used to characterize the different functionalizations of the halloysite surfaces as shown in Fig. 2. For all modifications, an increase in the weight loss after grafting was observed. These weight losses were attributed to the decomposition of the grafted organic parts which suggests, along with FTIR results, the efficiency of the functionalization procedures used. HNT-F and HNT-S show weight losses of about 1.2 and 0.4 wt%, respectively. Moreover, the second step of functionalization to obtain HNT-SF from HNT-S resulted in an additional increase in the weight loss of about 1.2 wt% attributed to the fluorinated grafting agent.

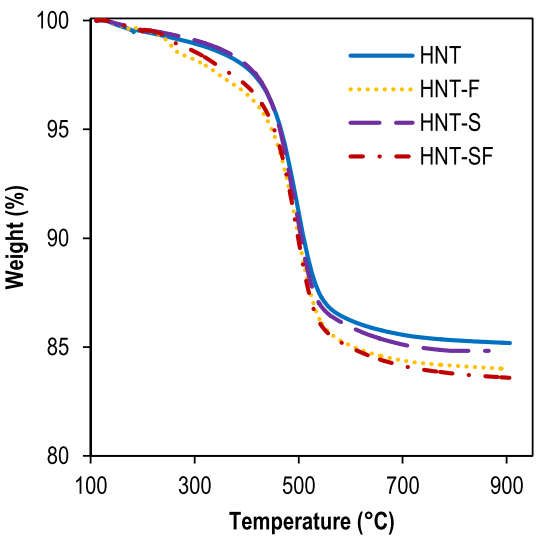

Figure 2 TGA under nitrogen of pristine halloysite, HNT-F, HNT-S and HNT-SF samples from 110 to 900 °C after an isotherm at 110 °C for 10 min.

The amount of functional groups in HNT-F, HNT-S and HNT-SF are approximately 2.3×10^{-5} mol/g, 1.7×10^{-5} mol/g and 4×10^{-5} mol/g, respectively. Moreover, the surface area of halloysite used in this work is 64 m^2/g thus grafting rate per surface area can be calculated. 3.5×10^{-7} mol/m^2, 2.7×10^{-7} mol/m^2 and 6.3×10^{-7} mol/m^2 of grafting rate were obtained for HNT-F, HNT-S and HNT-SF, respectively.

Finally, Py–GC/MS was used to verify the different functionalization of halloysite. The analyses used a pyrolysis step at 900 °C to evaluate the presence and the nature of the organic molecules on the filler's surface after the grafting procedures. The results obtained for HNT-F, HNT-S and HNT-SF (see Fig. 3) confirmed the presence of the grafting agents after the halloysite functionalization, whereas no peak was observed for pristine halloysite, chromatograms of functionalized clays show peaks corresponding to organic molecules obtained by thermal degradation of the grafted parts. The presence of fluorinated molecules was observed for HNT-F and HNT-SF due to the release of fluorinated molecules by decomposition of the fluorinated grafting agent. Different aromatic molecules were observed for HNT-S due to the thermal decomposition of the naphthalene part of the grafting agent. We have to notice that when a multi-grafting procedure was used as for HNT-SF, the obtained chromatogram shows essentially a peak due to the fluorinated part. This can be due to relatively lower grafting rate obtained with the sulfonic grafting agent as observed from TGA results.

Based on the above description, Py–GC/MS analysis confirmed the presence of the grafting agents on the modified halloysite nanotubes after the grafting procedures.

In terms of further work, we need more characterization to evaluate if some *N*-(3-triethyoxysilylpropyl)perflurooctanoamide molecules outcompete the sulfonated molecule used during the first step of the grafting procedure. Moreover, the intensity of the peaks for Py–GC/MS spectra depends on the quantity of molecule but it is not possible to directly compare two different peaks and estimate the difference in quantities depending on the difference in intensity.

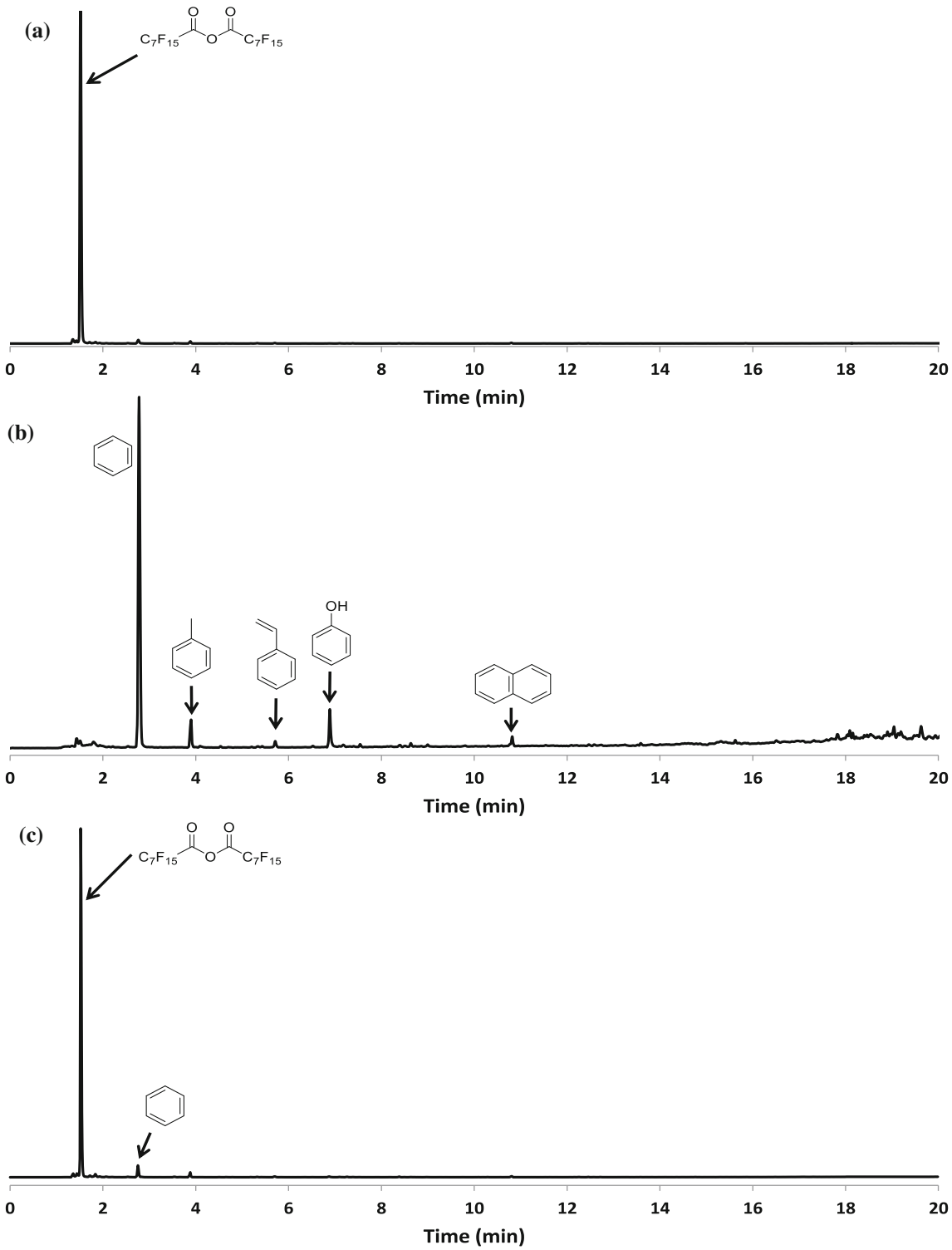

Figure 3 Py–GC/MS chromatograms obtained for **a** HNT-F, **b** HNT-S and **c** HNT-SF samples pyrolyzed at 900 °C.

Membrane characterization

Thickness of electrolyte membranes

The membrane thickness is considered as a crucial characteristic to reduce the ohmic losses during PEMFC operation [49], often at the expense of a higher hydrogen crossover. To achieve the benefits, the membrane thickness was targeted to 20 μm at room temperature and dry conditions. The state-of-the-art membrane Nafion HP is approximately 20 μm thick, in dry conditions, a value close to that measured using FE-SEM for pristine Aquivion membrane prepared in this work. All data are displayed in Fig. 4a, b (dry state), (hydrated condition).

The thickness of dehydrated Aquivion, Aq/HNT-F10, Aq/HNT-S10 and Aq/HNT-SF10 membranes is close to the expected values: 24.6 ± 0.7, 24.5 ± 0.3, 22.7 ± 0.3 and 20.6 ± 0.7 μm, respectively (see Fig. 4a). Aq/HNT10 on the contrary was about 13 μm thicker than expected (i.e., 33.3±0.9 μm) most probably due to halloysite aggregation inside the polymer phase as can be seen in Fig. 5d. This may result from the presence of voids between the halloysite particles or poor interface between the fillers and Aquivion.

Composite membranes blended with pretreated halloysites were also similar to the targeted thickness, i.e., around 20 μm in dry state. The pretreatment did not impact the dispersion of the fillers, and the composite membranes are rather homogeneous.

The membranes prepared in this study were immersed in DI-water to be recovered from the glass plate they are prepared on. The membrane thickness was subsequently measured in wet state. Results are reported in Fig. 4b.

The thickness of hydrated Nafion HP was measured 23 μm.

Pristine Aquivion membrane was slightly thicker (32 μm) compared with the selected commercially available membrane.

As expected, the incorporation of halloysite, pristine or modified resulted in thicker composite membranes, between 40 and 54 μm. The reason is that halloysite expands upon water absorption and intercalation. This is because halloysite is in the form of a tube, thus this structure is easy to expand the thickness of composite membranes incorporated with 5 wt% clay nanoparticles. As another cause, halloysite constriction might be occurred in the membranes containing 2 and 10 wt%, but further work can be considered for the exact cause. Accordingly, halloysite concentration may lead to variation in membrane thickness.

Figure 4 Data on **a** dehydrated thickness, **b** wet thickness, **c** water uptake, **d** ion exchange capacity (IEC), **e** swelling ratio at room temperature between dry and wet states and **f** swelling ratio in wet state between room temperature and 100 °C: commercially available Nafion HP and pristine Aquivion and Aquivion composite membranes containing various halloysites, HNT, HNT-F, HNT-S and HNT-SF. Yellow and blue bars represent non-pretreated and pretreated nanoclays Aquivion composite membranes, respectively. ▶

Again, the thickest membrane (54 μm) was obtained with 10 wt% pristine halloysite (Aq/HNT10). That is, functionalized nanoclays led to thinner membranes due to a better dispersion, and probably better interaction with Aquivion, than pristine halloysite, more agglomerated.

The pretreatment of halloysites in oxalic acid and hydrogen chloride has a very limited impact on the thickness, regardless of functionalization type and nanoclay content (2 wt%, 5 wt%, and 10 wt%). The only exception is Aq/pHNT10 (10 wt% of pretreated halloysite) whose thickness is equal to that of our pristine Aquivion membrane.

Water uptake

The proton transfer is affected by water molecules inside the ionomer matrix according to Grotthuss and vehicle mechanisms [49, 50]. The water uptake is an essential property to evaluate the proton transfer in PEMFC application.

As shown in Fig. 4c, the water uptake of the Aquivion membrane (38%) was slightly higher than that of the Nafion HP (30%).

Due to their hygroscopicity, the addition of 10 wt% halloysite in Aquivion clearly resulted in an increase in water uptake.

Comparing 10 wt% loaded composites prepared with the same type of halloysite, it is clear from Fig. 4c that the pretreatment has a limited impact on the water uptake. The amount of fillers seems to impact the water uptake of pretreated halloysites. A continuous increase in the water uptake with the amount of clay nanotube was expected. However, a maximum was reached for 5 wt% loading, whatever the type of functionalization, reaching values

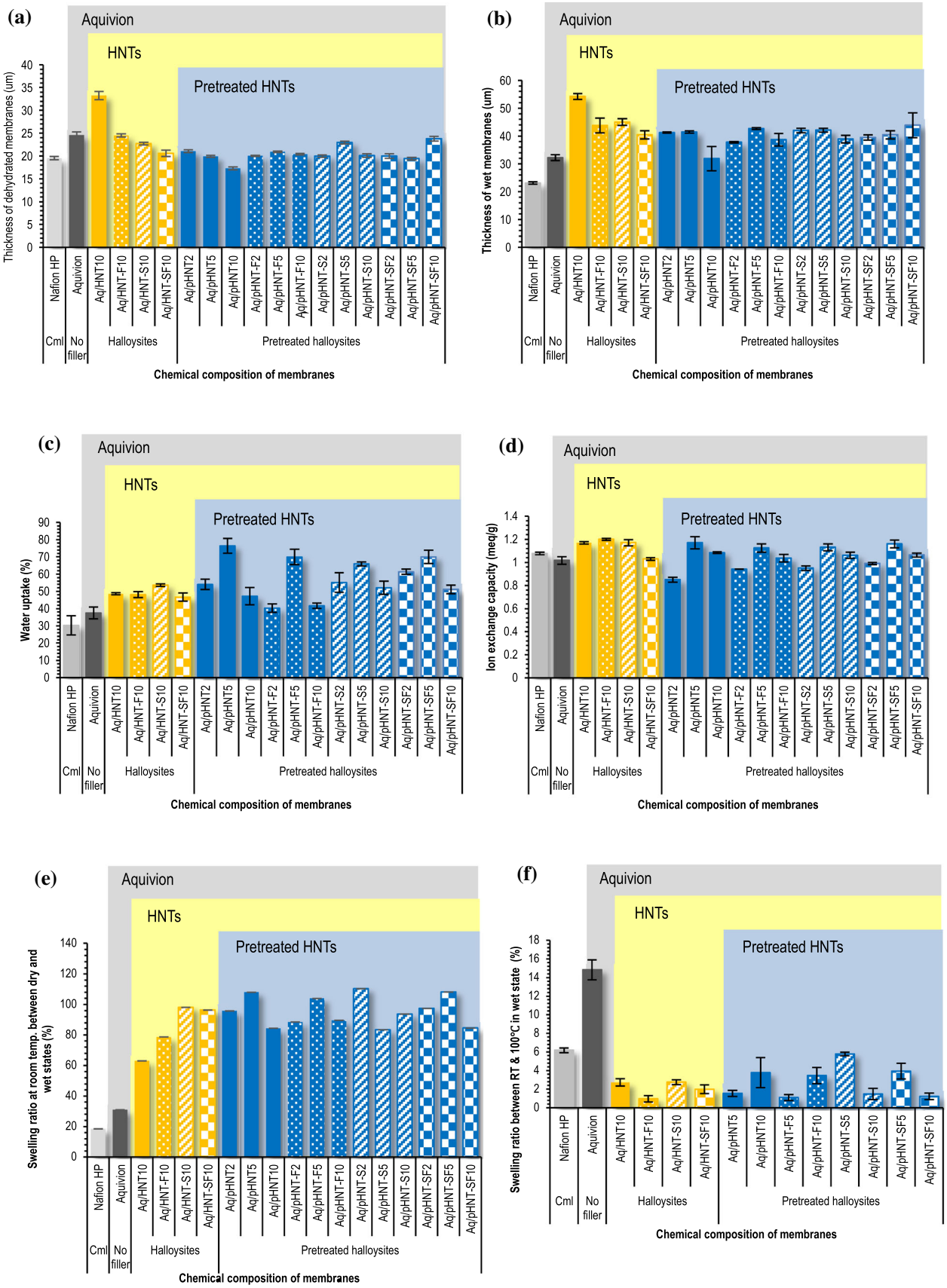
(a)
Aquivion
HNTs
Pretreated HNTs
Thickness of dehydrated membranes (um)
Nafion HP
Aquivion
Aq/HNT10
Aq/HNT-F10
Aq/HNT-S10
Aq/HNT-SF10
Aq/pHNT2
Aq/pHNT5
Aq/pHNT10
Aq/pHNT-F2
Aq/pHNT-F5
Aq/pHNT-F10
Aq/pHNT-S2
Aq/pHNT-S5
Aq/pHNT-S10
Aq/pHNT-SF2
Aq/pHNT-SF5
Aq/pHNT-SF10
Cml
No filler
Halloysites
Pretreated halloysites
Chemical composition of membranes
(b)
Aquivion
HNTs
Pretreated HNTs
Thickness of wet membranes (um)
Chemical composition of membranes
(c)
Aquivion
HNTs
Pretreated HNTs
Water uptake (%)
Chemical composition of membranes
(d)
Aquivion
HNTs
Pretreated HNTs
Ion exchange capacity (meq/g)
Chemical composition of membranes
(e)
Aquivion
HNTs
Pretreated HNTs
Swelling ratio at room temp. between dry and wet states (%)
Chemical composition of membranes
(f)
Aquivion
HNTs
Pretreated HNTs
Swelling ratio between RT & 100°C in wet state (%)
Chemical composition of membranes

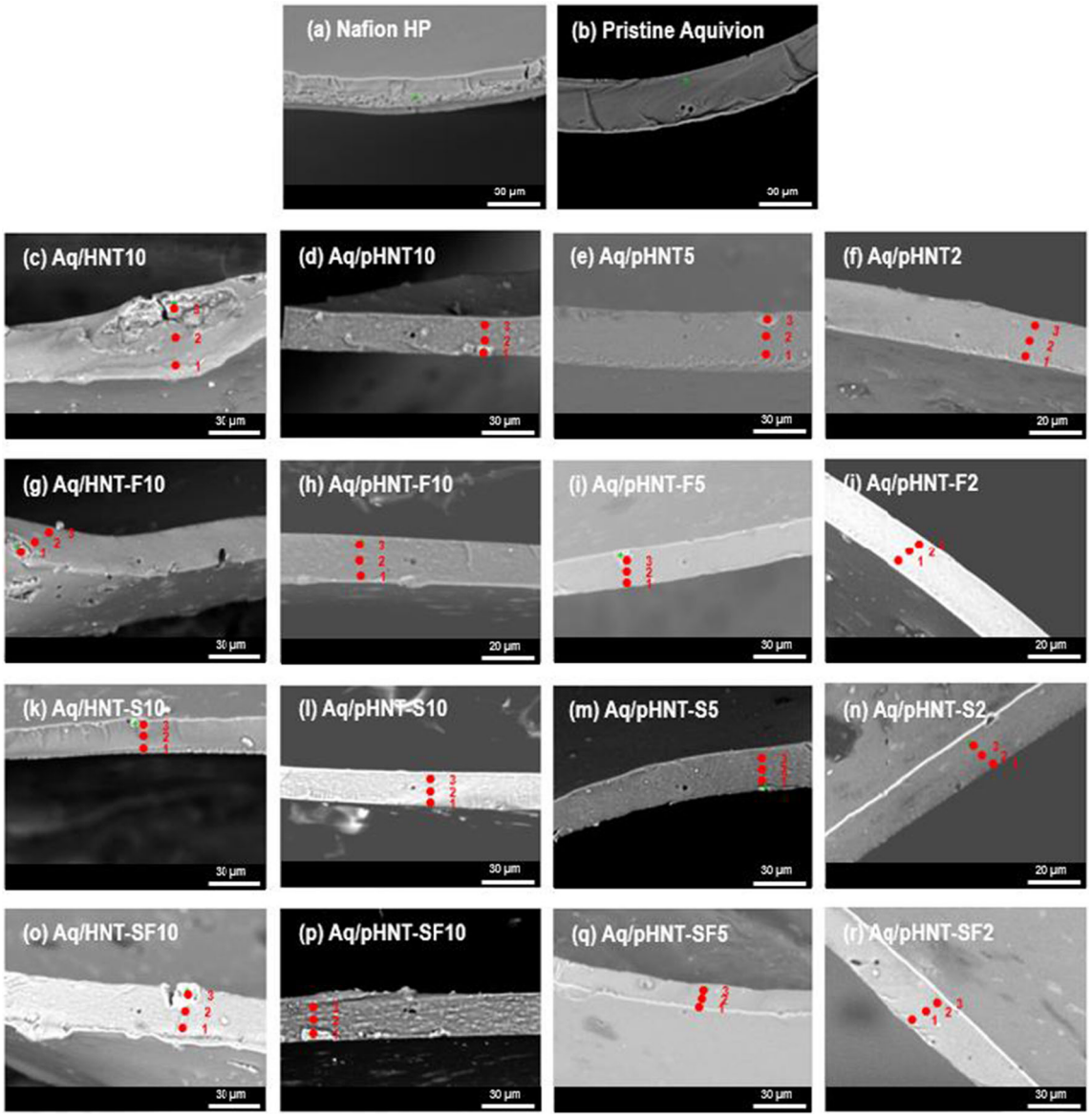

Figure 5 FE-SEM images regarding **a** commercially available Nafion HP, **b** pristine Aquivion, and **c**–**r** Aquivion composite membranes blended with HNT, HNT-F, HNT-S and HNT-SF. The images are available in the online version of the paper.

between 65 and 75%. This implies that functionalization can lead to an improvement in water uptake and accordingly impacts the proton conductivity of the membranes.

Dimensional properties

Figure 4e, f displays the swelling behavior of the different membranes, which is another crucial feature for fuel cell performance since it is related to mechanical properties and thermal stability.

Pristine Aquivion showed similar dimensional properties between dry and wet states at room temperature (calculated with Eq. (2)), 26% versus 29%. Nafion HP on the contrary exhibited a much smaller value of 2%.

Whatever the type of halloysite, pristine or modified, pretreated or not, a much higher swelling behavior was observed for composite membranes compared to pristine Aquivion membranes, + 100% for 10 wt% pristine HNT, + 150% for HNT-F and + 200% for HNT-S and HNT-SF. In agreement with the evolution of the water uptake, the pretreatment did not seem to have any impact on this swelling for 10 wt% loaded membranes, whereas a maximum was

observed for 5 wt% added pHNTs (except for sulfonated ones). Further work may be required to understand the reason why pHNT-S-loaded membranes display different trends in swelling ratio at room temperature as compared to other membranes. Depending on the dispersion direction of pHNT-S nanoclay inside membranes, swelling might impact the membrane surface area (width × length) more than the membrane thickness.

Figure 4f shows that the influence of the temperature on the swelling of wet membranes is completely different. Generally speaking, this swelling between room temperature and 100 °C was significantly less (one order of magnitude) than the swelling at room temperature described above.

Our pristine Aquivion membrane showed by far the largest swelling among the membranes tested. Nafion HP membrane was less subjected to swelling in such conditions.

The addition of 10 wt% halloysites tremendously reduced the thickness swelling of all composite membranes, from 15% for Aquivion to about 4% for composites, regardless of functionalization. This is attributed to a reinforcement caused by the 1D morphology of halloysite nanotubes as discussed in former publications [26, 37, 42]. The fluorination may have a positive effect since Aq/HNT-F10 and, in a lower extent, Aq/HNT-SF10 membranes showed lower swelling.

The pretreatment had no significant impact. After pretreatment of various halloysites, the composite membranes still showed rather limited swelling values, between 1.1 and 5.8%.

No real trend could be drawn either concerning the amount of pretreated clay nanotube. A decrease from 10 to 5 wt% entailed a swelling increase after pretreatment for unmodified and fluorinated halloysites, whereas it raised for sulfonated and perfluoro-sulfonated ones. Hence, the evolutions observed cannot be considered as representative.

Ion exchange capacity

IEC is a crucial property for ionomers, related to the number of ion exchange groups. It affects the proton conductivity of PEMs according to Grotthuss theory [51]. The IEC of commercially available, pristine and composite membranes displayed values between 0.94 and 1.20 meq/g, as shown in Fig. 4d. The addition of nonionic conductive nanoclays may affect the apparent IEC value of the corresponding composite membrane.

Except for perfluorosulfonated halloysite, the addition of halloysite (pristine, fluorinated, or sulfonated) resulted in slightly higher IEC. The pretreatment has a limited impact on the IEC which is for 10 wt% added pretreated halloysite (modified or not) only slightly lower (5–10%) compared to that obtained with non-pretreated clays. As previously observed, for pretreated clay nanotubes, the amount of fillers seems to impact the IEC, higher IECs being once again obtained for 5 wt%. Large amounts (10 wt%) of clay nanotubes may block the side chain of the Aquivion thus isolating the sulfonic groups, which is in good agreement with reduced water uptake (see Fig. 4c) and ionic conductivity (see Fig. 11) of 10 wt% nanoclay-incorporated composite membranes.

Homogeneity of composite membranes

A uniform distribution of the fillers across the membrane is expected to decrease the interaction with charges crossing the membrane from the anode side to the cathode side, thus improving the proton movement. Additional impacts on both the thickness and the mechanical strength of the membranes are expected. Figure 5 shows FE-SEM cross section of the different membranes investigated, the commercially available one and those prepared according to "Membrane preparation" section. Both edge of membranes and the center of the cross section were chemically analyzed in order to get insights on the nanoclay repartition across the membrane thickness. Silicon and fluorine originating from halloysite and Aquivion were, respectively, considered as markers to discuss about the distribution of nanoclays inside the polymer phase.

Blending of pristine halloysite with Aquivion displays large aggregates, compared with that of functionalized halloysites as shown in Fig. 5c, g, k, o. If the functionalization of halloysite allowed to largely avoid the formation of agglomerates, it hardly impacted the fine repartition of the nanoclay within the polymer matrix. Indeed, the Si/F atomic ratio of all the composite membranes, calculated from EDS results, differs from one side to the other of the membranes. Concerning 10 wt% loaded composites, similar values have been moreover obtained (between 15 and 18 at the edges of cross section),

regardless of functionalization as shown in yellow bars of Fig. 6. In general, the pretreatement of halloysite resulted in a significative improvement of the nanoclay repartition within the membrane. The difference of Si/F between both sides is divided by a factor of two. The effect is more pronounced with sulfonated and perfluorosulfonated halloysites, the latter resulting even in quite homogenous composites.

The amount of added clay nanotubes does not impact the homogeneity of the composite whatever the type of nanoclay.

Dynamic mechanical analysis (DMA)

DMA tests were performed in order to evaluate the influence of the different functionalization types on the storage and loss modulus, respectively G' and G''.

For all membranes tested, the storage modulus initially increased with the temperature, up to 90 or 100 °C. This may result from the elimination of water remaining in the membrane, leading to a stiffening of the membrane before the glass transition domain.

It is also shown that up to 120 °C, composite membranes containing non-pretreated and functionalized HNT have a lower storage modulus than the unmodified HNT one (see Fig. 7a). Those non-pretreated HNT composite membranes are interesting because they maintain their stiffness (especially Aq/HNT-SF10) to very high temperatures, much higher than pristine Aquivion. As a result, the glass transition temperature (Tg) of the composite membranes is significantly shifted to higher temperature (see Fig. 7c), probably to around 180 °C for Aq/HNT10, Aq/HNT-F10 and Aq/HNT-S10 and even much higher for Aq/HNT-SF10.

The pretreatment of halloysite, modified or not, resulted in a slight modification of the mechanical properties. Indeed, the stiffness of all composite membranes was increased (see Fig. 7b), whereas their glass transition temperature was decreased (see Fig. 7d). The latter remained however higher than that of pristine Aquivion (170 °C vs. 140 °C).

Chemical stability

PFSA membranes can be chemically degraded by free radicals such as hydroxyl HO·and hydroperoxyl HOO attacking the C–F bonds during operation of hydrogen fuel cells. This ultimately affects the thickness and consequently the permeability of the membrane, resulting in an increase in H_2 crossover. It has been reported that iron oxide is naturally present in halloysites [52–54]. Iron ions may then react with H_2O_2 to form OH radicals which eventually degrade the ionomer and the membrane [8, 55–57]. To assess the chemical stability of the prepared membranes and the possible role of such intrinsically present iron ions, they were immersed in H_2O_2/H_2SO_4 solution at 80 °C up to 96 h. The concentration of fluoride ions eventually released upon Fenton reaction in the solution was measured after 48, 72 and 96 h of

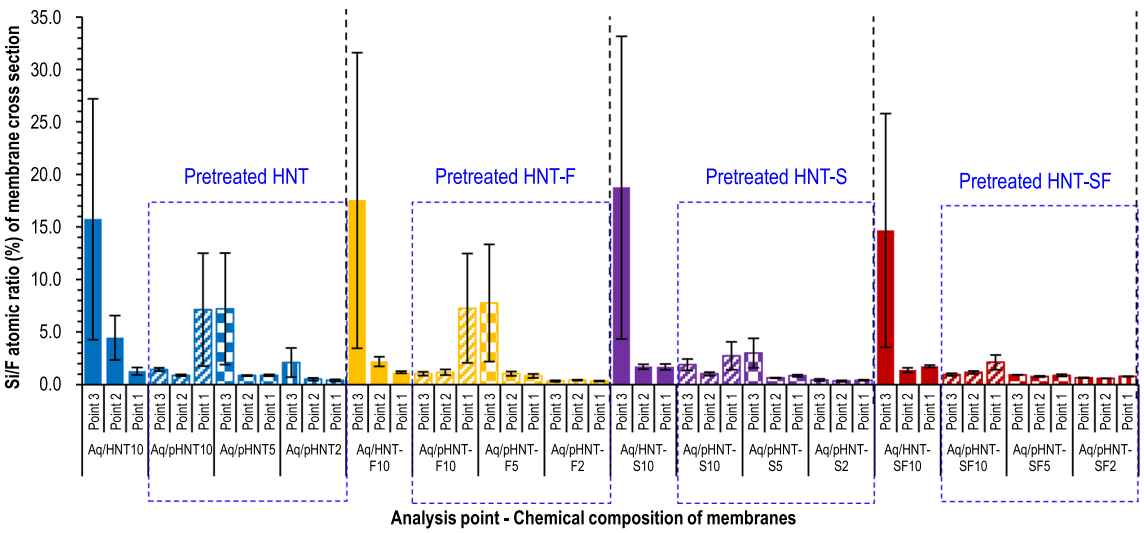

Figure 6 Si/F atomic ratio calculated from EDS measurements recorded on pristine Aquivion and Aquivion composite membranes incorporated with HNT, HNT-F, HNT-S and HNT-SF. Patterns represent pretreated nanoclays.

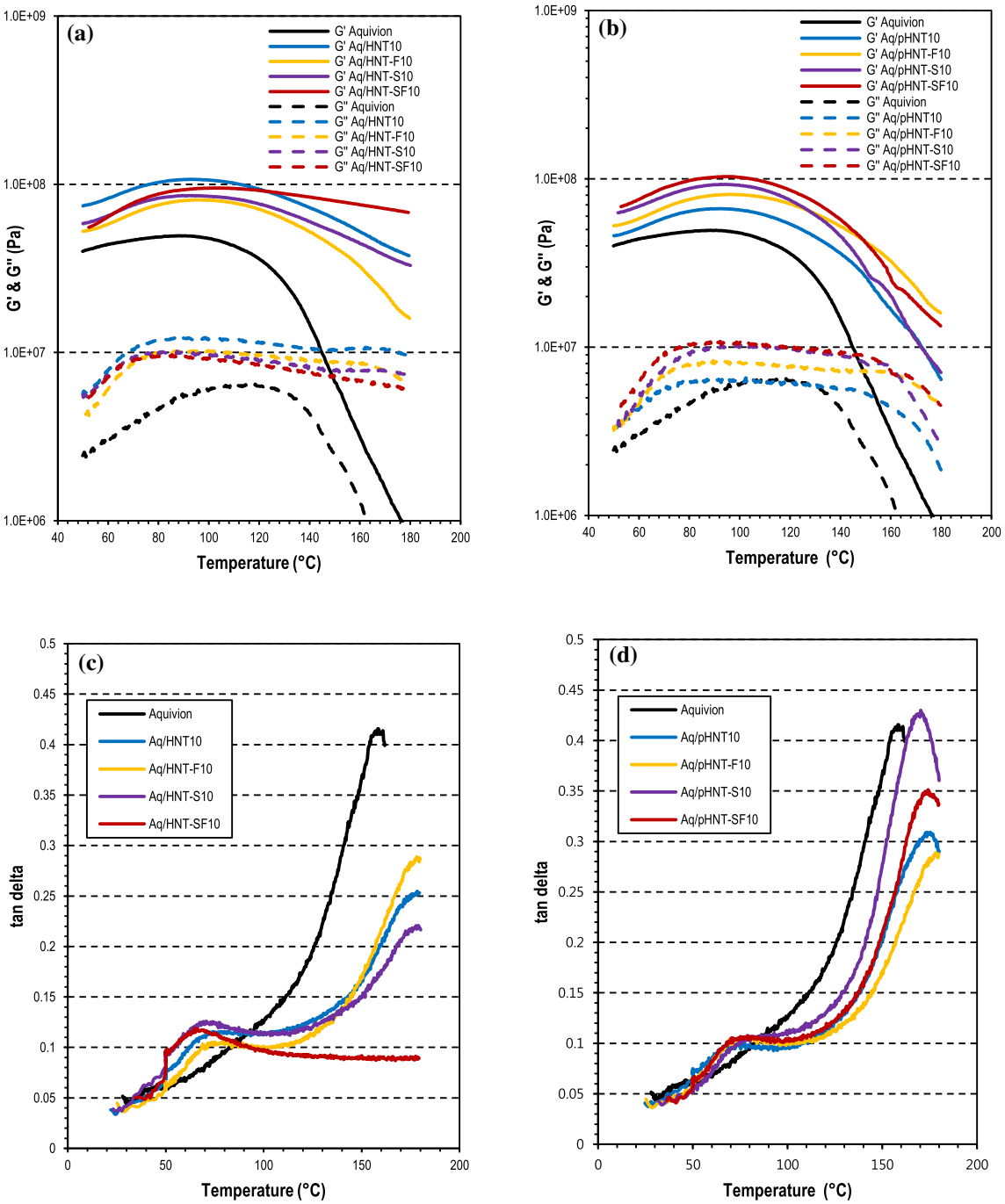

Figure 7 DMA results on G' and G'' of Aquivion and composite membranes containing 10 wt% of **a** non-pretreated and **b** pretreated HNTs. DMA data on tan delta of electrolyte membranes blended with 10 wt% of **c** non-pretreated and **d** pretreated HNTs.

immersion. For all the studied membranes, the fluoride ion concentration increased with the immersion time (see Fig. 8).

The pristine Aquivion membrane exhibited less chemical stability than commercial membrane Nafion HP. Those commercial membranes most probably contain some antioxidant components which make them more chemically stable.

Reducing the amount of halloysite did not impact the fluorine concentration. Either the concentration measured can be considered as negligible or the amount of iron in the 2 wt% loaded composites is

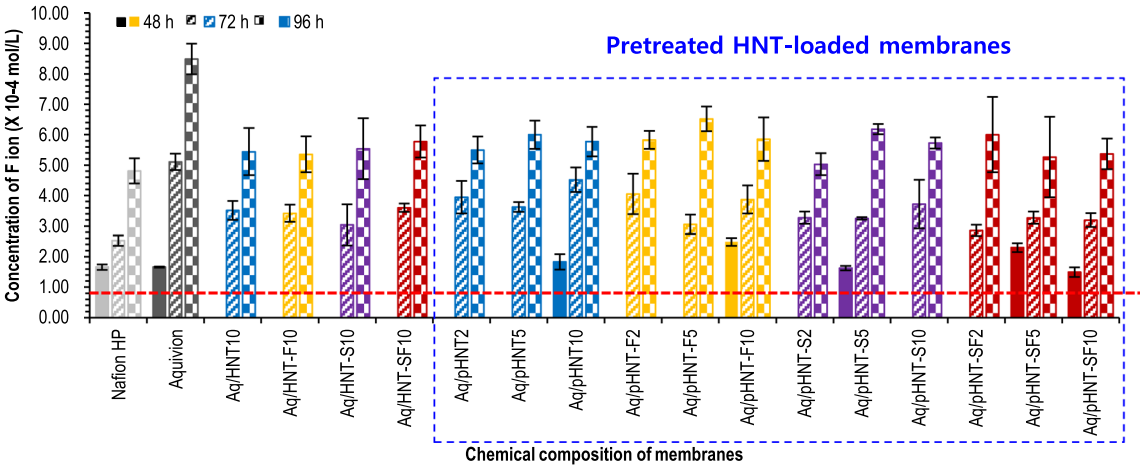

Figure 8 Fluoride (F^-) concentration analyzed after immersion in H_2O_2/H_2SO_4 for Nafion HP, pristine Aquivion, Aq/HNT, Aq/HNT-F, Aq/HNT-S, Aq/HNT-SF, Aq/pHNT, Aq/pHNT-F, Aq/pHNT-S and Aq/pHNT-SF membranes. Red dotted line represents the fluorine concentration of 4.4 M H_2O_2/1.25 mM H_2SO_4 solution (blank test): $0.82 \times 10^{-4} \pm 0.08 \times 10^{-4}$ mol/L.

already large enough to contribute to the degradation, even if limited.

The role of the pretreatment was to remove most of the iron from the halloysite. However, the composite membranes with pretreated halloysites released similar fluoride concentrations to those without pretreatment. The reason can be explained by EDS results, evidencing a limited removal of iron upon pretreatment (Fig. 9). For future experiments, if necessary, a stronger and more effective pretreatment process may be required to remove excess divalent iron from halloysites, i.e., those which are not structural and responsible for the tubular structure of HNT.

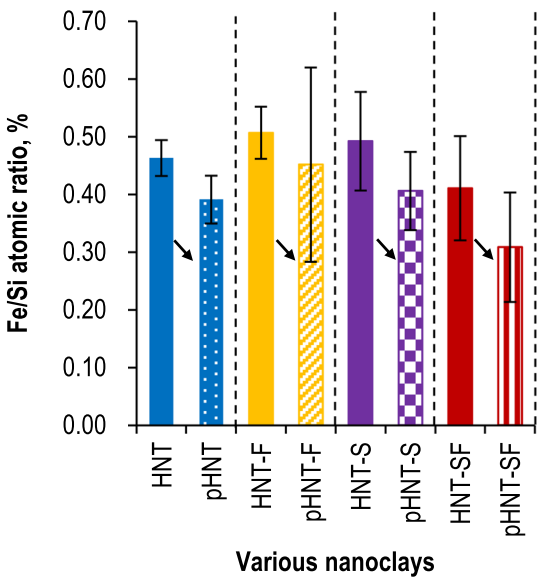

Figure 9 Comparison of Fe/Si atomic ratio (%) regarding HNT, pHNT, HNT-F, pHNT-F, HNT-SF, pHNT-SF, HNT-S and pHNT-S clay nanotubes used for preparing composite membranes. Patterns represent pretreated nanoclays.

Proton conductivity

In the study, the through-plane proton resistance of each membrane was measured using impedance spectroscopy in various conditions of temperatures (50 °C, 70 °C, and 90 °C) and relative humidity (25%, 50%, 75%, and 90%). The low ohmic resistance obtained through the EIS results indicates that the fuel cell performance is likely to be good in a wide range of operating conditions.

Figures 10 and 11 display the proton conductivity calculated with Eq. (5) using the thickness of each membrane measured in the wet state.

Pristine Aquivion with shorter side chains than Nafion led to higher proton conductivity. Larger crystallinity of Aquivion can also lead to higher proton conductivity than long side chain PFSA of similar EW [2, 3].

The proton conductivity of all composite membranes prepared with non-pretreated halloysites (HNT-10, HNT-F10, HNT-S10 and HNT-SF10) was relatively low compared to that of the pristine Aquivion membrane.

Composite membranes with pretreated nanoclays displayed improved proton conductivity, except in the case of pure halloysite. The incorporation of non-functionalized HNTs in Aquivion was already

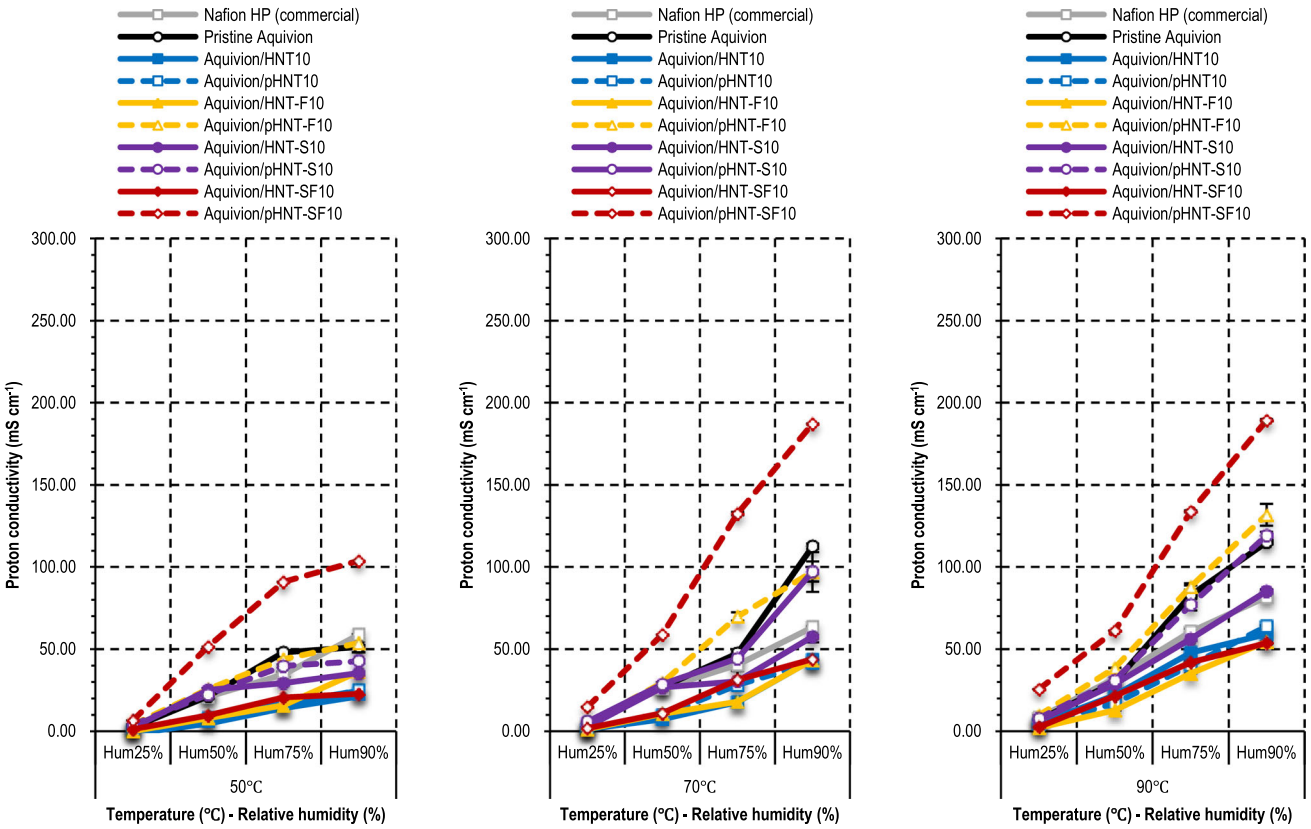

Figure 10 Proton conductivity comparison of non-pretreated and functionalized versus pretreated and functionalized nanoclays-based composite membranes under various temperature and relative humidity: Nafion HP, pristine Aquivion, Aquivion/HNT, Aquivion/HNT-F, Aquivion/HNT-S, Aquivion/HNT-SF, Aquivion/pHNTs, Aquivion/pHNTs-F, Aquivion/pHNTs-S and Aquivion/pHNTs-SF composite membranes incorporated with 10 wt% contents. Blue, yellow, purple, and red lines represent pristine HNT, fluorinated HNT, sulfonated HNT, and perfluorosulfonated HNT, respectively. Solid and dashed lines represent non-pretreated and pretreated HNTs, respectively.

reported to lead to a significant decrease in conductivity, which was ascribed to the poor dispersion of the fillers [43]. The enhanced proton transfer in membranes loaded with the functionalized nanoclays can be thus explained with the improvement of the filler dispersion resulting in more homogeneous composite membranes without perturbation of the nanostructure and of the ion transport channels. The pretreatment process had an overall positive influence, but the results varied depending on the functional group at the clay surface. In the case of fluorinated or sulfonated halloysite only, the proton conductivity reached the level of pristine Aquivion. The double functionalization, sulfonation plus fluorination, allowed to increase even more the proton conductivity compared to pristine Aquivion. Among the membranes tested, blending of pretreated and perfluoro-sulfonated halloysite exhibited the highest proton conductivity, overpassing that obtained with Aquivion.

pHNT-SF was the most efficient clay nanotube to increase the proton conductivity. The impact of its content was then studied and the proton conductivity of the resulted membranes compared to that of a selection of external and internal reference membranes (see Fig. 11).

It is clear once again from Fig. 11 that whatever the clay content, 2, 5 or 10 wt%, the pretreatment of HNT-SF is very beneficial to the proton conductivity of the composite membranes. Higher proton conductivities, compared with pristine Aquivion and Nafion HP, were obtained for 5 wt% pretreated and perfluoro-sulfonated HNT (pHNT-SF5)-contained composite membrane at 50–90 °C. Moreover, it is in fact always greater than that of composite membranes prepared with pristine halloysite (HNT),

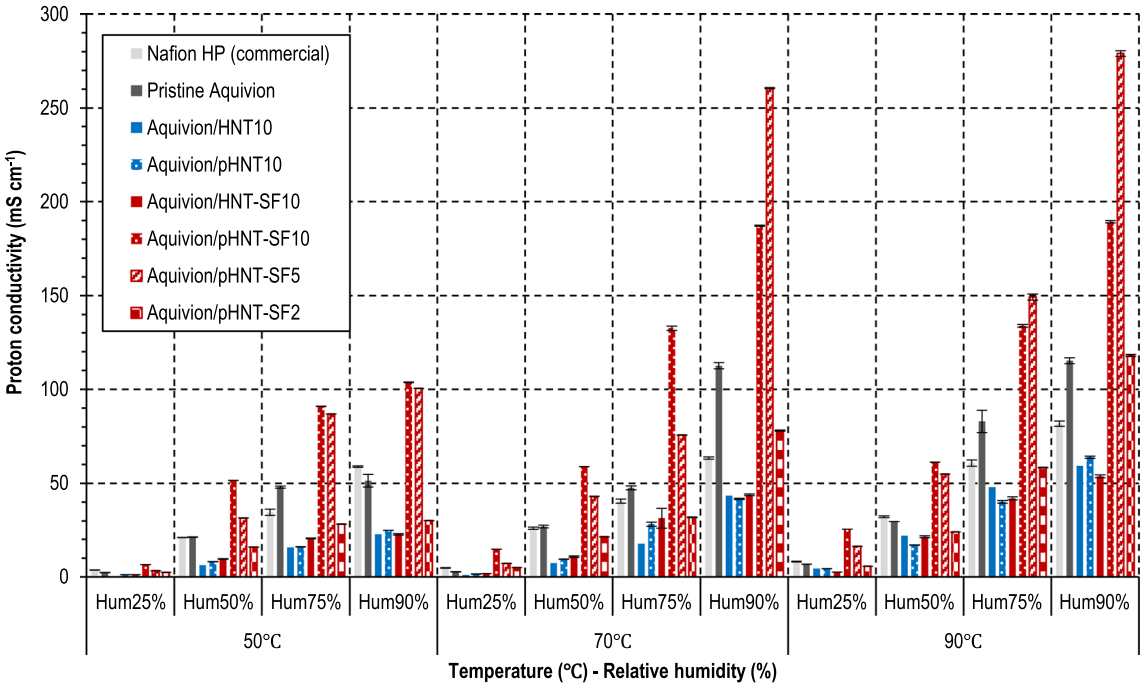

Figure 11 Influence of the pHNT-SF content (2, 5, and 10 wt%) in Aquivion on the proton conductivity under different temperatures and relative humidities. Comparison with Nafion HP, pristine Aquivion, Aquivion/HNT-10, Aquivion/pHNT-10.

perfluoro-sulfonated HNT (HNT-SF) or pretreated HNT (pHNT10).

Consistently with data obtained on IEC and water uptake, the highest proton conductivity, 280 mS cm^{-1}, was reached with 5 wt% pHNT-SF at 90 °C and 90%RH.

Conclusions

Halloysite nanotubes were selectively modified with fluorinated, sulfonated, or perfluoro-sulfonated groups grafted on the inner or outer surface of the tubes. Different Aquivion composite membranes were prepared by casting of a mixture of these modified clays with a commercial Aquivion suspension. Their physicochemical properties were characterized and compared with those of Nafion HP.

Blending pure halloysite into Aquivion phase resulted in improved water uptake, swelling and mechanical properties. The composite membrane not only displayed similar IEC, but also showed reduced proton conductivity compared to Nafion HP.

Functionalized clay nanotubes resulted in stiffer (for Aq/HNT-SF10) and thinner composite membranes than pure halloysite. Similar composite homogeneity, swelling, chemical stability, water uptake and IEC were obtained, regardless of functionalization types.

The pretreatment associated with the functionalization of halloysites proved to be beneficial to the composite homogeneity and the proton conductivity. In particular, the incorporation of 5 wt% pretreated and perfluoro-sulfonated halloysite (i.e., pHNT-SF5) into Aquivion matrix led to the highest proton conductivity among the membranes tested. Moreover, Aq/pHNT-SF10 was particularly interesting as it displayed improved mechanical property (better stiffness). Moreover, according to the fluoride ion concentration, the pretreatment did not affect the chemical stability as expected.

The amount of pretreated and functionalized halloysite nanotubes is impacting the IEC, the water uptake and the proton conductivity with a maximum reached for 5 wt%. In particular, the influence for Aq/pHNT-SF5 was noticeably impressive, compared with commercially available Nafion HP as far as proton conductivity is concerned.

Based on a large set of characterization techniques, it is suggested that improved physicochemical properties of Aquivion/pretreated and perfluoro-sulfonated halloysite electrolyte membrane have a

potential in PEMFC operation, under a wide range of conditions.

Acknowledgements

This study was supported by funding under the COMEHTE project (Contract Number ANR-15-CE05-0025-01) Granted from French National Research Agency (ANR). The authors wish to thank Patrick Leroux (PERSEE center), Pierre Ilbizian (PERSEE center), Cedric Sernissi (PERSEE center), Suzanne Jacomet (CEMEF center) Gabriel Monge (CEMEF center), Loïc Dumazert (C2MA center) and Benjamin Gallard (C2MA center) for technical support. SC acknowledges IUF for financial support. This work was partly supported by Korea Evaluation Institute of Industrial Technology (KEIT) grant funded by the Korea government (MOTIE) (1415173267, Development of UF membrane for separation and concentration of proteins).

References

[1] Feng K, Liu L, Tang B, Li N, Wu P (2016) ACS Appl Mater Interfaces 8:11516–11525
[2] Li J, Pan M, Tang H (2014) RSC Adv 4:3944–3965
[3] Stassi A, Gatto I, Passalacqua E et al (2011) J Power Sources 196:8925–8930
[4] Subianto S, Pica M, Casciola M et al (2013) J Power Sources 233:216–230
[5] Aricò A, Di Blasi A, Brunaccini G et al (2010) Fuel Cells 10:1013–1023
[6] Yang Z, Nakashima N (2016) ChemCatChem 8:600–606
[7] Dupuis A-C (2011) Prog Mater Sci 56:289–327
[8] Peighambardoust S, Rowshanzamir S, Amjadi M (2010) Int J Hydrog Energy 35:9349–9384
[9] Kim DJ, Jo MJ, Nam SY (2015) J Ind Eng Chem 21:36–52
[10] Kongkachuichay P, Pimprom S (2010) Chem Eng Res Des 88:496–500
[11] Şengül E, Erdener H, Akay RG, Yücel H, Bac N, Eroğlu İ (2009) Int J Hydrog Energy 34:4645–4652
[12] Tripathi BP, Kumar M, Shahi VK (2009) J Membr Sci 327:145–154
[13] Carbone A, Saccà A, Gatto I, Pedicini R, Passalacqua E (2008) Int J Hydrog Energy 33:3153–3158
[14] Nagarale R, Shin W, Singh PK (2010) Polym Chem 1:388–408
[15] Mishra AK, Bose S, Kuila T, Kim NH, Lee JH (2012) Prog Polym Sci 37:842–869
[16] Zhengbang W, Tang H, Mu P (2011) J Membr Sci 369:250–257
[17] Matos B, Aricó E, Linardi M, Ferlauto A, Santiago E, Fonseca F (2009) J Therm Anal Calorim 97:591–594
[18] Di Noto V, Gliubizzi R, Negro E, Pace G (2006) J Phys Chem B 110:24972–24986
[19] Pereira F, Vallé K, Belleville P, Morin A, Lambert S, Sanchez C (2008) Chem Mater 20:1710–1718
[20] Jalani NH, Dunn K, Datta R (2005) Electrochim Acta 51:553–560
[21] Saccà A, Carbone A, Pedicini R et al (2008) Fuel Cells 8:225–235
[22] D'Epifanio A, Navarra MA, Weise FC et al (2009) Chem Mater 22:813–821
[23] Zhai Y, Zhang H, Hu J, Yi B (2006) J Membr Sci 280:148–155
[24] Subianto S, Donnadio A, Cavaliere S et al (2014) J Mater Chem A 2:13359–13365
[25] Filippov A, Khanukaeva D, Afonin D et al (2015) J Mater Sci Chem Eng 3:58–65
[26] Cavallaro G, De Lisi R, Lazzara G, Milioto S (2013) J Therm Anal Calorim 112:383–389
[27] Oroujzadeh M, Mehdipour-Ataei S, Esfandeh M (2015) RSC Adv 5:72075–72083
[28] Fernandez-Carretero FJ, Suarez K, Solorza O, Riande E, Compan V (2010) J New Mater Electrochem Syst 13:191–199
[29] Bébin P, Caravanier M, Galiano H (2006) J Membr Sci 278:35–42
[30] Chang J-H, Park JH, Park G-G, Kim C-S, Park OO (2003) J Power Sources 124:18–25
[31] Nicotera I, Enotiadis A, Angjeli K, Coppola L, Gournis D (2012) Int J Hydrog Energy 37:6236–6245
[32] Mura F, Silva R, Pozio A (2007) Electrochim Acta 52:5824–5828
[33] Woo SH, Taguet A, Otazaghine B, Mosdale A, Rigacci A, Beauger C (2019) Electrochim Acta 319:933–946
[34] Beauger C, Lainé G, Burr A, Taguet A, Otazaghine B, Rigacci A (2013) J Membr Sci 430:167–179
[35] Beauger C, Lainé G, Burr A, Taguet A, Otazaghine B (2015) J Membr Sci 495:392–403
[36] Bao X, Zhang F, Liu Q (2015) Int J Hydrog Energy 40:16767–16774
[37] Liu X, He S, Song G et al (2016) J Membr Sci 504:206–219
[38] Bielska D, Karewicz A, Lachowicz T, Berent K, Szczubiałka K, Nowakowska M (2015) Chem Eng J 262:125–132
[39] Zhang H, He Y, Zhang J, Ma L, Li Y, Wang J (2016) J Membr Sci 505:108–118
[40] Zhang H, Ma C, Wang J, Wang X, Bai H, Liu J (2014) Int J Hydrog Energy 39:974–986

[41] Ressam I, El Kadib A, Lahcini M, Luinstra GA, Perrot H, Sel O (2018) Int J Hydrog Energy 43:18578–18591
[42] Zhang H, Zhang T, Wang J, Pei F, He Y, Liu J (2013) Fuel Cells 13:1155–1165
[43] Akrout A, Delrue A, Zatoń M et al (2020) Membranes 10:1–18
[44] Rico-Zavala A, Gurrola M, Arriaga L et al (2018) Renew Energy 122:163–172
[45] Woo SH, Rigacci A, Beauger C (2019) Chem Lett 48:418–421
[46] Zatoń M, Rozière J, Jones D (2017) SUT J Math 1:409–438
[47] Healy J, Hayden C, Xie T et al (2005) Fuel Cells 5:302–308
[48] Yuan P, Southon PD, Liu Z et al (2008) J Phys Chem C 112:15742–15751
[49] Agmon N (1995) Chem Phys Lett 244:456–462
[50] Grancha T, Ferrando-Soria J, Cano J et al (2016) Chem Mater 28:4608–4615
[51] Zhao C, Lin H, Shao K et al (2006) J Power Sources 162:1003–1008
[52] Joussein E, Petit S, Churchman J, Theng B, Righi D, Delvaux B (2005) Clay Miner 40:383–426
[53] B Szczepanik, P Słomkiewicz, M Garnuszek et al (2015) J Mol Struct 1084:16–22
[54] Szczepanik B, Rogala P, Słomkiewicz PM, Banaś D, Kubala-Kukuś A, Stabrawa I (2017) Appl Clay Sci 149:118–126
[55] Guo Q, Pintauro PN, Tang H, O'Connor S (1999) J Membr Sci 154:175–181
[56] Büchi FN, Gupta B, Haas O, Scherer GG (1995) Electrochim Acta 40:345–353
[57] Xie J, Wood DL, Wayne DM, Zawodzinski TA, Atanassov P, Borup RL (2005) J Electrochem Soc 152:A104–A113